
Original Paper

Study of surface changes on industrial glasses with AFM, FE-SEM, EDX, SNMS and LM

Part 1. Glass skin and corrosion

Chun Wang, Wolfgang Häfner and Georg Krausch
Physikalische Chemie II, Universität Bayreuth, Bayreuth (Germany)

Edda Rädlein
IMA I, Universität Bayreuth, Bayreuth (Germany)

Stephan Tratzky
SCHOTT-Rohrglas GmbH, Mitterteich (Germany)

Manfred Schramm
Bayerische Flaschen-Glashüttenwerke Wiegand & Söhne GmbH & Co. KG, Steinbach am Wald (Germany)

Klaus-Peter Martiněk
FX Nachtmann Bleikristallwerke GmbH, Riedlhütte (Germany)

By combining different analytical techniques, including modern high resolution imaging tools such as field emission scanning electron microscopy (FE-SEM) and atomic force microscopy (AFM), new phenomena in the surface, near surface and bulk structure of various industrial glasses (without any cleaning process) have been discovered. Investigations of soda-lime-silica container glass and lead silicate glass tubings exposed to atmospheric and to dried air are presented. The results of the first part of this paper can be explained with an SiO₂-rich skin on the glass, which can protect the glass against the attack of external media. If the skin was mechanically injured, inhomogeneous corrosion products on µm scale grew around the injured site after exposure to humid air for times between days up to one year. Microchannels were formed through the injured site due to restricted ion exchange, followed by a local increase of the pH value and consequently the dissolution of the glass network. Finally some stress in the glass, yielded during manufacture, can be partially released and the cutting behaviour is improved. Faster cooling results in a thinner skin and the ions in the glass are able to migrate to the surface more easily when surrounded by some reactive media. Slower cooling results in thicker skin and wax-like droplets instead of crystallites are formed on the surface at a later stage in humid air. The wax-like droplets can etch the glass skin locally, followed by the growth of inhomogeneous corrosion products similar to the injury induced corrosion. If the fresh glass surface was hot-end treated, the quality of the adjacent coating layer depended strongly on the thickness of the skin.

1. Introduction

The commonly accepted structure of silicate glass is a continuous random network, constructed by SiO₂. Usually, different oxides are introduced into the SiO₂ matrix to meet specific requirements concerning their physical and/or chemical properties. Some oxides are glass formers, fixed in the glass network; some oxides are network modifiers, with a certain mobility between the network meshes. The surface

properties of glasses depend strongly on the chemical composition and the structure of glass. They depend also on the surrounding media. The humid atmosphere is the most common surrounding medium to result in changes on glass surface [1 and 2]. The attack of the glass surface by moisture can be classified into three types. Type 1 consists of the diffusion-controlled process of a proton or a hydronium anion from water penetrating into the glass network, replacing an alkali ion. The alkali ion in turn diffuses to the glass surface and reacts with the atmospheric carbon dioxide and water molecules resulting in corrosion products. At this stage, the silica network remains unchanged, but at a later stage, following a continuous ion exchange, the pH value on the surface might increase up to pH > 9. Then the decompo-

Received 8 September 2003.

Presented in German at: 77th Annual Meeting of the German Society of Glass Technology (DGG) on 28 May 2003 in Leipzig (Germany).

sition of the silica network starts. Type 2 is the development of coordinative binding of the OH group from water to the Si atom in glass, resulting in a gel layer on the glass surface. Type 1 and Type 2 are irreversible attacks of moisture. Type 3 is a physical adsorption. Water molecules attach to the Si–OH groups and result in a water film on the glass surface, which gives rise to change of the surface properties. Type 3 is reversible and can be removed by drying the sample at higher temperature and/or in vacuum [3 and 4].

However, every solid state object has a pristine surface, which differs from bulk, due to inhomogeneous surroundings of the surface atoms and the tendency to lower the surface energy. If the glass surface is melt-formed in a gaseous medium, the perfectly smooth surface of a liquid is frozen in. Formerly one believed that the surface was cooled faster than the bulk, so the surface should have a lower refractive index corresponding to a lower density, because of a disordered structure frozen in the surface layer. Later some researchers observed, however, that the glass surface was covered by a higher refractive index layer of about 4 nm [3]. The results of our work agree with the latter. We named this layer a glass skin. It influences the mechanical, chemical and physical properties of glass evidently, especially the quality of an adjacent coating. The glass skin protects the glass against the attack of surrounding media, but it can also result in inhomogeneities of the glass surfaces. In this paper we discuss the observations related to the glass skin on microdiode tubings made from lead silicate glass and on drink bottles made from soda-lime-silica glass.

2. Experimental

2.1 Samples

All the samples were industrial products. The glass surfaces were not treated with any cleaning process. The microdiode tubings were manufactured from lead silicate glass with a PbO content of 60 wt%. The drink bottles were made of white, green and brown soda-lime-silica glass. Some samples were taken from the assembly line and put into an exsiccator for transport to the laboratory, some samples were taken from the store room in industry. The samples for FE-SEM investigations, except the broken surfaces of the microdiode tubings, were fractured and coated with carbon to avoid charging of the insulating glass surfaces.

2.2 Methods of analysis

The surface, near surface and bulk structures were revealed by using light microscopy (LM, Axiovert, Carl Zeiss Jena GmbH, Jena (Germany)), atomic force microscopy in height mode (AFM, NanoScope Dimension 3100, Digital Instruments, Santa Barbara, CA (USA)) and field emission scanning electron microscopy (FE-SEM, LEO 1530, Carl Zeiss NTS Inc., Oberkochen (Germany)). The FE-SEM device is equipped with three detectors: a) the InLens detector collects the secondary electrons coming directly from the spot centre on the outmost surface at lower accelerating voltages of 0.5 to 2 kV to show the surface morphology of samples, b) the SE 2 detector collects the secondary electrons from deeper region at higher accelerating voltages of above 5 kV to show the near surface structure, and c) the

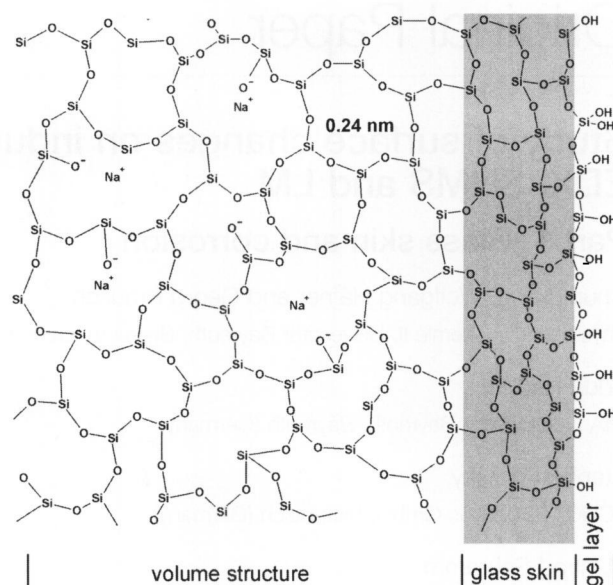


Figure 1. Schematic presentation of the glass network structure near a surface.

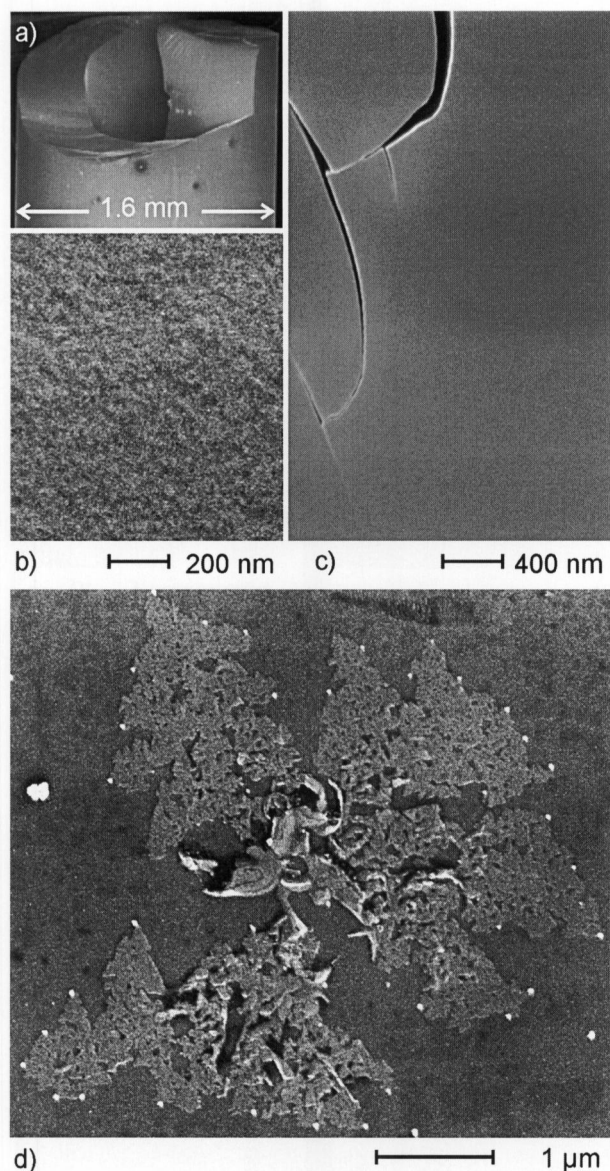
Table 1. Comparing the sizes of some atoms and groups, which may be involved in the glasses studied

	six SiO ₂ tetrahedra	H ₂ O	Na atom	K atom	Al atom	Pb atom	Ca atom
Ø in nm	0.24	0.28	0.34	0.43	0.26	0.24	0.34

RBS detector collects the backscattered electrons at voltage of 7 to 20 kV to show the material contrast images. The chemical compositions of the samples were determined with energy dispersive X-ray spectrometry (EDX, INCA 400, Oxford Instruments, Concord, MA (USA)) equipped on the FE-SEM instrument. The element depth profiles of the samples were recorded by using secondary neutral mass spectrometry (SNMS, INA 3, Leybold AG, Köln (Germany)).

3. Results and discussion

Many evidences of glass surfaces confirmed that glass has a higher density skin. It can be considered that glass network is like a fishnet. On the margin, the net mesh can not be completely extended due to lack of three dimensional drawing forces. Such configuration deformation results in smaller net voids. In addition, it has been reported that the glass surface is formed mainly by three or four silicate tetrahedra [5], whilst the volume is formed by six-, seven- and eight-membered rings [6]. Such construction results in additional smaller net voids in the surface layer than in volume. A network unit of six-membered ring (where the ring opening is 0.24 nm) is comparable in size to the water molecule (0.28 nm) [6 to 8]. Based on our understanding, a schematic presentation of the glass network structure near the surface was drawn in figure 1. The gel layer (5 to 10 nm) consists of surface silanol groups and water molecules con-



Figures 2a to d. FE-SEM micrographs (Inlens, 1 kV) of a lead silicate microdiode tubing stored in air for one year; a) surveying picture, b) broken surface without carbon coating, c) inside and d) outside of the tubing after carbon coating.

nected through hydrogen bonds to the silanol groups. This layer can be formed in air within several minutes [9]. The skin formed through the configuration and construction deformations of the network should consist mainly of SiO_2 similar to a silica glass, because the ions are not able to exist in this region due to space requirement (table 1). Recent unpublished studies show that the root mean square (rms) roughness of a fresh glass skin can be as small as 0.14 nm ($(1 \times 1) \mu\text{m}^2$ image), which is similar to the rms roughness (0.1 nm) of an insulation glass fiber surface reported in literature [10]. The broken surface, no matter how flat it is, can not be as smooth as the skin surface.

Figures 2a to d show FE-SEM micrographs of different surfaces of a microdiode tubing. Figure 2a was taken on a terminal of a tubing with an unprecise cutting edge to serve as an illustration of each side investigated. Figure 2b shows a higher resolution image of a mirror smooth area of a

freshly broken surface of a tubing. The broken surface shows an irregular fluctuation pattern similar to many broken surfaces of other glass systems [11 and 12]. The diode tubing contains about 60 wt% PbO , which makes the glass conductive. The broken surface of the tubing can be scanned by SEM without any conductive coating, regardless whether fresh or aged, however the inside and outside of the tubing can not be imaged without conductive coating. This evidence brings up the hypothesis of the existence of an insulating, SiO_2 -rich skin at the glass surface. Figure 2c shows the melt-formed inside of a tubing (contacted only with gaseous media during the course of solidification). It is so smooth that no features could be observed. The distinct features of the broken and melt-formed surfaces in figure 2b and 2c display clearly different properties between the volume and surface of the sample. The rougher broken surface can be explained by the existence of inhomogeneities within the glass such as density fluctuations and alkali microsegregation [13]. The breaking occurs predominantly along the boundaries between the network and the modifier channels and the density of the network varies from place to place, so the broken surface of glass can never be as flat as the melt-formed surface.

The aim of this investigation has been to explore the reasons for the varying cutting behaviour of the tubings. Usually, aged tubings show "good cutting behaviour", resulting in flat cutting sections and precise length of the tubings. The "bad cutting ware" is usually newly produced and shows irregularly broken surfaces. The relaxation of the network at room temperature can be neglected due to the higher glass transition temperature of this sample. Another possibility to result in changes of the cutting behaviour might be the corrosion reactions of the glass in air. After numerous observations it has been found that the inside of all tubings does not exhibit features like wax-like droplets (observed often on soda-lime-silica glasses) no matter how long they have been exposed to humid air. The outside of the tubings shows many artifacts, like cordlines, scratching traces, dirty pieces etc., but only the good cutting wares have additional inhomogeneously crystallized corrosion products on the surfaces as shown in figure 2d. The flat plateau feature of the corrosion products is about 5 nm in height. The aggregates in the centre are as high as 50 nm (AFM measurement). The entire corrosion product has well defined edges and can be as large as several micrometers. Bright particles of approximately 50 nm in size are found around the contour of the corrosion appearance. They seem to stop the growth of the corrosion crystals. The shape of the crystal is trigonal with a size of 100 nm in the flat area, over several hundred nanometers stacked in the centre. The corrosion growth on the tubings is difficult to explain by the classic interpretation. Formerly it has been described that the ions (Na^+ , K^+ etc.) migrate via ion exchange with H_3O^+ or H^+ to the glass surface and into the gel layer. If the ions were supersaturated in the gel layer, crystals grew spontaneously or by a dust particle as a nucleus [9]. Such a phenomenon has been observed on the surface of lead crystal glass and on the air side of soda-lime-silica float glass after the samples being exposed to humid air over half a year (not shown here). In case of the microdiode tubings, the corrosion crystals are not observed everywhere and the aggregates in the centre are unusually high. The mechanism of the crystal growth can be described as follows: Both sides of the tubing are covered by an SiO_2 -rich skin with smaller

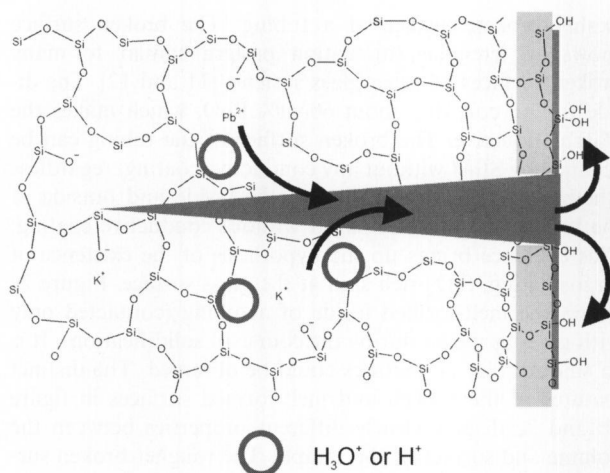
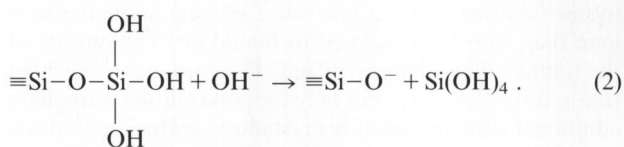
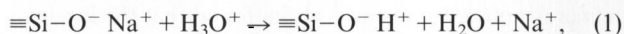


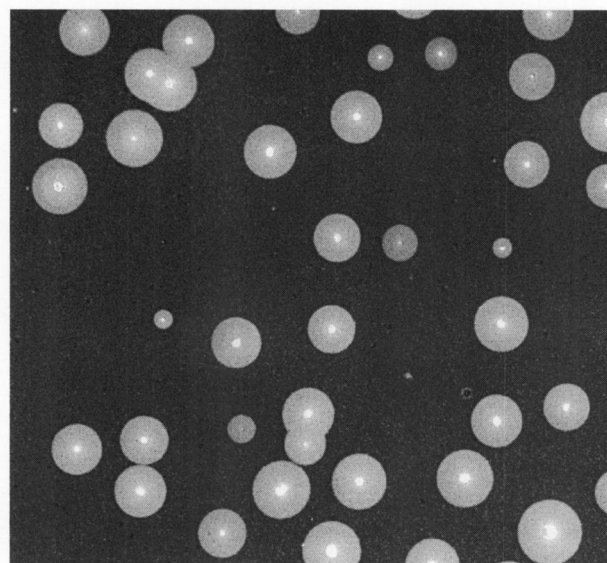
Figure 3. Schematic drawing of a microchannel yielded by corrosion process.

network voids. If the skin is undisturbed, it is able to protect the glass against attack of surrounding media for a long time, as shown in figure 2c. If the skin is injured, ion exchange takes place preferentially at the injured site, associated with an increasing of pH value. Above pH 9, the glass network is dissolved. The broken network in turn promotes further ion exchange at this site. After many cycles of ion exchange and network breaking, a microchannel is formed as shown in figure 3. The chemical reactions of ion exchange and network dissolution can be schematically described as follows [8]:

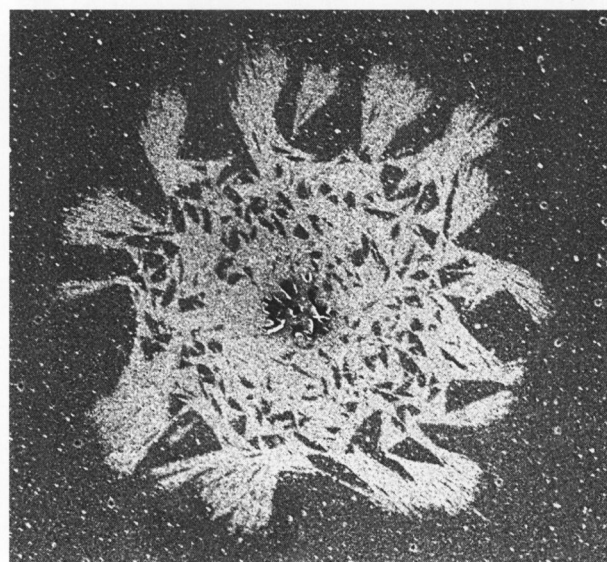


In fact, as early as 1978 Hench and Clark observed a preferential attack of water molecules at the surface scratches, when those were deeper than 0.2 μm [14], but they did not explain this observation clearly. Their observation corresponds to our description above. The numerous channels in the glass could release some stress built up during the production process. In consequence, the cutting behaviour of the sample might be improved. The tubings exposed to air for one year are usually “good cutting tubings“. But not the ageing time is the deciding factor, the essential criterion is whether corrosion products are formed on the glass surfaces. In other words, the release of the internal stress is responsible for good cutting behaviour.

Figures 4a and b give other examples of the inhomogeneous growth of corrosion products on the μm scale. Figure 4a shows an inside of a green soda-lime-silica glass bottle, which has round bright spots larger than 10 μm after being exposed to air for one week. Every spot has a protruding centre. Enlarged micrographs show that the centre consists of crystalline particles, which serve as entries to permit the water molecules to diffuse into the glass. The diffusion spots can only be imaged with a low accelerating voltage of



a) 40 μm



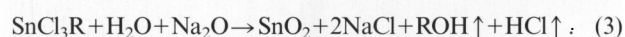
b) 4 μm

Figures 4a and b. FE-SEM micrographs (Inlens) of soda-lime-silica drink bottles showing inhomogeneous appearances of corrosion products on μm scale; a) inside of a green bottle exposed to air for one week (2 kV), b) inside of a brown bottle exposed to air for four weeks (1 kV).

FE-SEM (2 kV, Inlens). If the voltage increases up to 8 kV (the low limitation of normal SEM), no spots appear on the images. Lower voltage excites electrons in the outmost surface region, higher voltage excites electrons in deeper region. If more electrons are collected from the diffusion layer, the spot pattern emerges, if more electrons are collected from deeper regions, the spot pattern disappears. The inside of a brown bottle showed similar bright spots at the initial stage of corrosion (9 h, in air), if the glass skin was injured. After exposure to air over four weeks the spot developed into inhomogeneous corrosion products with dendrite pattern as shown in figure 4b. The dendrites may possibly be crystals of alkali and alkali earth carbonate species, investigated with Auger spectroscopy and infrared spectroscopy [14 and 15].

The formation mechanism of the inhomogeneous corrosion products in figures 4a and b should be similar to the case of microdiode tubing. Detailed description of various corrosion patterns, the composition of the products, the crystal forms and possible mechanisms in different glass systems are presently under investigation. From scientific consideration the injured skin is accidental, however from the industrial viewpoint the injured skin can not be avoided. We must bear in mind that glass surfaces exposed to ambient atmosphere at the production site exhibit inhomogeneous corrosion products on μm scale, which affect the bonding of coatings to silicate glass surface and result in bad adhesion of the final products, especially if the glass article has been stored in humid air for a long period.

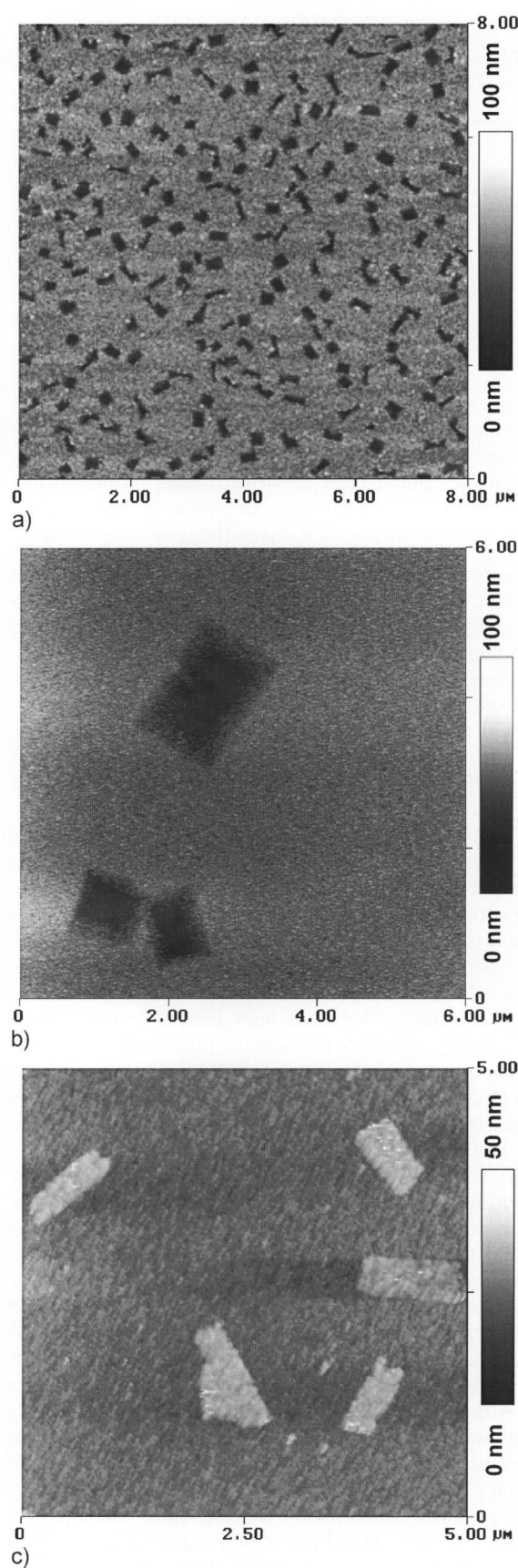
One of our industrial partners coats the outside of glass bottles with multilayers to obtain the required high strength at low container weight [16]. The first layer contacting the glass surface is prepared by hot-end coating with monobutyl tin chloride (SnCl_3R) vapour. Adhesion tests of the coating show that the failure position is within this first layer. AFM images in figures 5a to c reveal the morphology of the first layer, after an adhesion test on a multilayer coated white bottle (5a) and without other coatings on a brown bottle (5b and c). The rectangular holes in figures 5a and b are previously filled with rectangular crystallites as shown in figure 5c, which grew from the glass surface, but did not firmly adhere to it. By breaking the bottle into pieces to suit the AFM and FE-SEM measurements, most of the crystallites were skipped off. Fortunately, a small portion of the crystallites remained at the surface and could be imaged by AFM. The chemical reaction is described as:



The growth of crystallites in a hot-end coating SnO_2 layer on soda-lime-silica glass surface is schematically drawn in figure 6. The crystallites are composed of NaCl , which has been ascertained with a series of X-ray photographs in literature [17].

SnO_2 is a very stable material even at temperatures above 1100°C . In this work it formed a monograin layer (about 10 nm in size and 10 nm in thickness) to cover the fresh glass surface against attack of ambient media. The existence of NaCl crystallites is not expected. It is very important for the industry to understand that the crystallites are formed on white bottle rather than on brown bottle, and to find a method to improve the coating layers.

According to reaction (3), if Cl^- ions are able to capture Na^+ ions easily, more NaCl crystallites are formed. However, few crystallites could be formed. There is not much difference in the compositions of both bottles, especially concerning the Na_2O contents, but the cooling rates are very different. White bottles radiate heat much faster than brown bottles during production process. It is reasonable to believe that a thinner skin is formed on white bottles, because the network on the surface has not enough time to move into a suitable configuration to fit the surface requirement and the Cl^- ions reach the Na^+ ions more easily than in the case of brown bottles. In order to prove this hypothesis, a systematic investigation based on industrial products has been carried out. The cooling rates decrease in the sequence from white, green to brown bottles, from outside to inside, from quenching to normal cooling, from press-blow to blow-blow



Figures 5a to c. AFM images ($\mu\text{m} \times \mu\text{m}$) of the SnO_2 layers on the outsides of drink glass bottles with hot-end treatment; a) SnO_2 coating on white bottle after adhesion test, b) SnO_2 coating on brown bottle, c) remaining NaCl crystallites in SnO_2 layer on brown bottle.

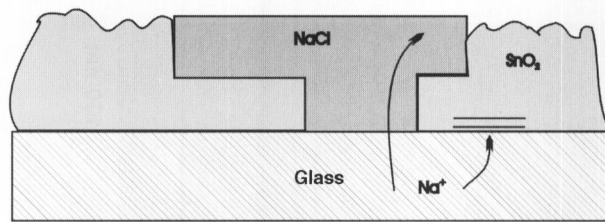
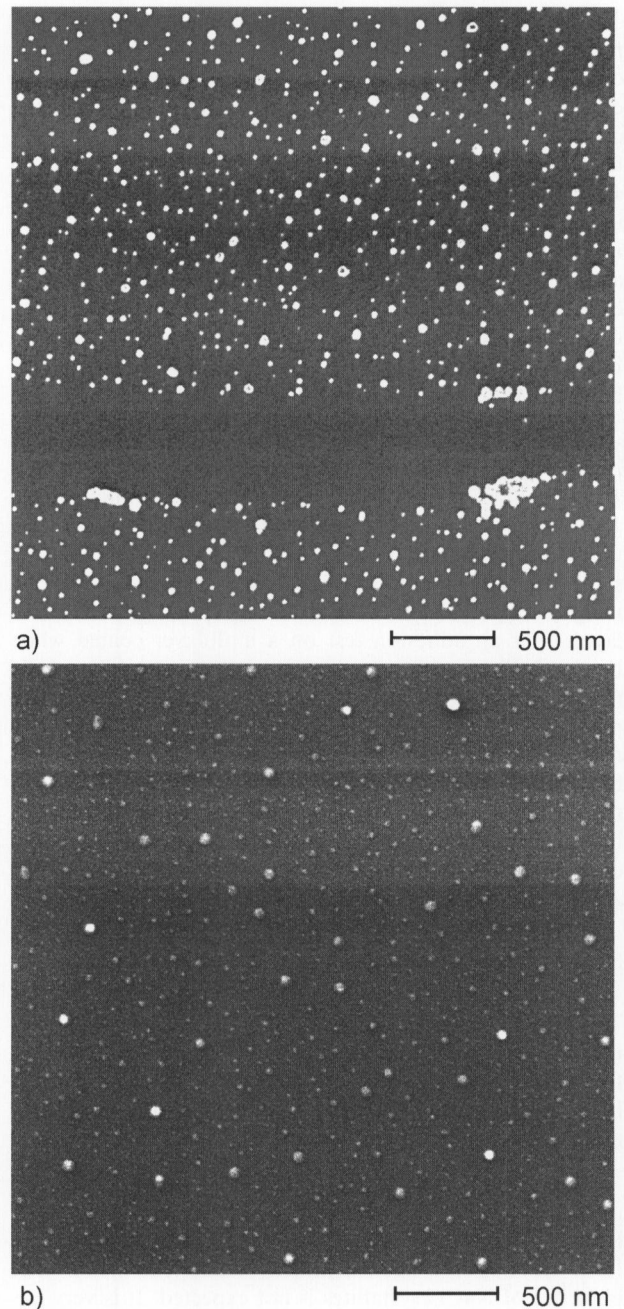


Figure 6. Schematic drawing of the formation of NaCl crystallite in hot-end coating layer on glass surface.

techniques. The combination of white bottle, outside, quenching process and press-blow technique should create a surface with the thinnest skin due to the fastest cooling rate and the combination of brown bottle, inside, normal cooling process and blow-blow technique should create a surface with the thickest skin due to the slowest cooling rate.

A series of FE-SEM investigations has ascertained that there is a morphology transition from crystallites to wax-like droplets on the various bottles corresponding to different cooling rates when they are exposed to air in the same conditions. The FE-SEM micrograph in figure 7a was taken on the outside of a green bottle prepared by quenching process, with press-blow technique. The entire surface is covered with crystallites in the size of 10 to 50 nm. The piled up crystallites in the corner clarify their solid state nature. This feature is similar to the outside of white bottles prepared by the same process. They belong to a faster cooling type. Figure 7b was taken on the inside of a brown bottle prepared by normal cooling and blow-blow technique. The entire surface is covered with wax-like droplets of comparable size to the crystallites in figure 7a. The outside of this brown bottle shows a similar pattern to the inside. These bottles belong to a slower cooling type. It is reasonable to believe that thinner skin has been formed in the case of faster cooling, which is not able to protect the Na^+ ions from the attack of water in air and Na^+ ions migrate onto the surface and react with CO_2 and water in air to form crystallites. If the skin is thick enough, the Na^+ ions are not easily reached by water molecules and no crystallites are formed. Only wax-like droplets are observed on the thicker skin surface as shown in figure 7b. As time passes the droplets are growing and change their shapes. Figure 8 is the FE-SEM micrograph of a droplet on the same sample as in figure 7b after exposure to air for four weeks. The centre of the droplet shows a depression and around the droplet there spreads a halo band. If the ageing time is even longer, dendrite corrosion crystals are growing from the halo band as in the case of figure 4b. Within the droplets water molecules react with the glass skin. At a late stage the glass skin is etched away. From that time on the Na^+ ions in the glass are able to easily migrate to the surface, which is comparable to injury corrosion. Consequently inhomogeneous corrosion products are formed. Washing away the wax-like droplets results in round holes with higher rims on the glass surface [18]. How to get a perfectly clean surface is still an open question. The long-time ageing of the faster cooling bottle in air shows different features from the slower cooling one. Figures 9a to c show the ageing investigations on the inside of a white bottle. At the beginning the surface is covered with crystallites showing the same behaviour as in the



Figures 7a and b. FE-SEM micrographs (Inlens, 0.5 kV) of the bottle surfaces showing the morphology on nm scale, a) outside of a green bottle, prepared by press-blow technique and quenched from red-hot state to room temperature, exposed to air for 9 h, b) inside of a brown bottle prepared by blow-blow technique and slower cooling (as normal production process) to room temperature, exposed to air for 9 h.

case of figure 7a. One year later, the crystallites have grown into larger ones with hexagonal shape. The different corrosion behaviour of faster cooling and slower cooling bottles has been expressed more clearly by the ageing process and may explain the different coating behaviour on the hot-end treated bottle surfaces as we have proposed previously. During the hot-end treatment, the thinner skin on the white bottle can not protect the Na^+ ions in glass against the rapid attack of the Cl^- ions in SnCl_3R vapour, and they react to form numerous NaCl crystallites on the

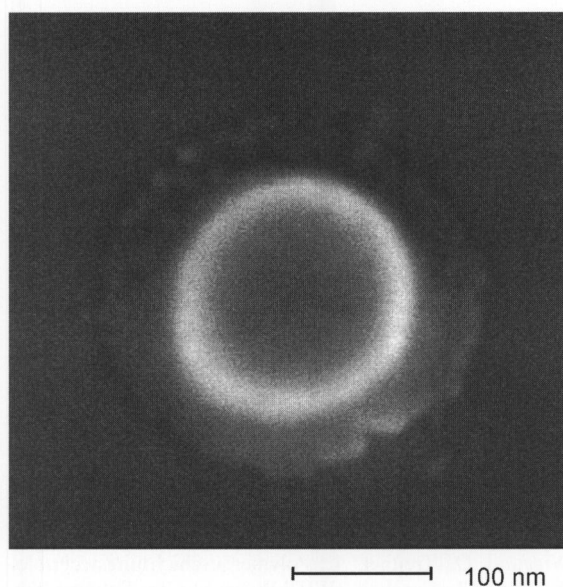


Figure 8. Development of a wax-like droplet on the same sample as in figure 7b, after exposure to air for four weeks.

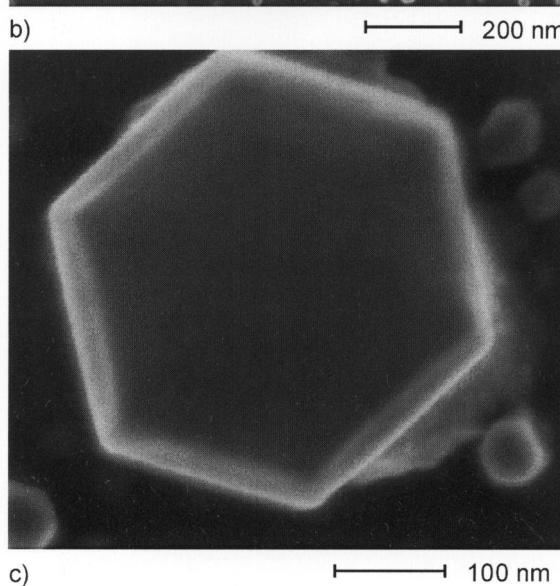
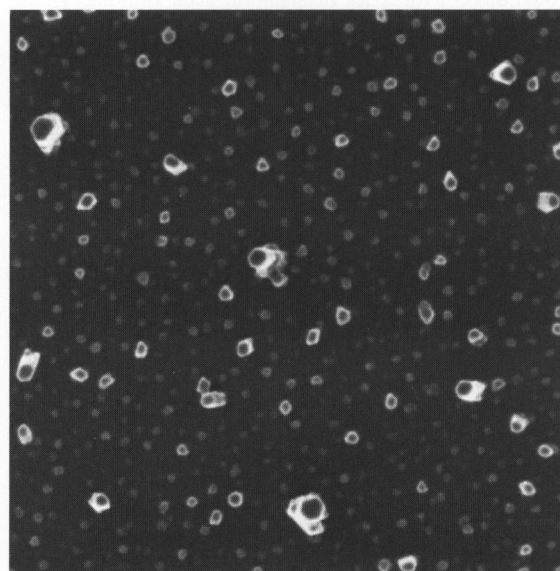
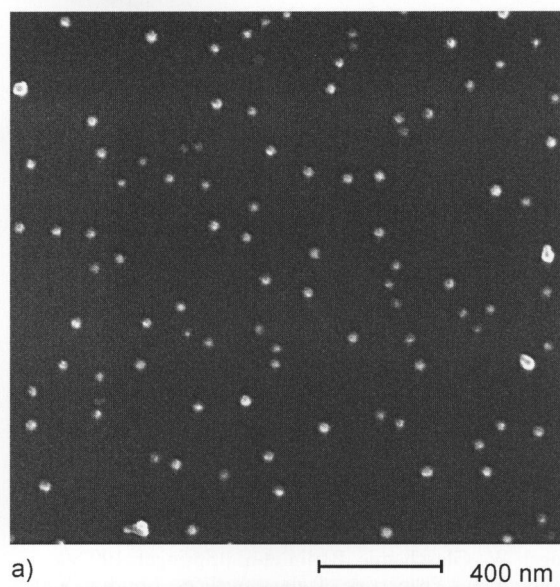
glass surface, whilst the thicker skin on the brown bottle provides a protective layer, so that few crystallites are formed. The corrosion behaviour and the coating behaviour are different only due to the different surrounding media attacking the fresh glass surfaces. So the skin thickness is very important for a high quality coating.

Formerly, the SiO_2 -rich layer related to a cooling rate has also been noticed. It was explained with the ion evaporation process [19 and 20]. By slower cooling, more ions escaped from glass into atmosphere and left a thicker SiO_2 -rich layer on the surface. This is a possible reason for a skin to be formed. But configuration deformation seems to be the major cause, because the skin is not only SiO_2 rich, but has also a very small roughness and a higher density compared to the bulk. If the skin is worn away, dramatic changes in the surface feature take place, which have been observed on the surfaces of glass articles after dishwasher treatment. Still existing skin islands in the size of hundred μm appeared brilliant and flat with roughness value of $\text{rms} \approx 1.5 \text{ nm}$, whereas skinless area near the skin islands showed honeycomb-like feature and the roughness value was as high as 12 nm (unpublished work). This phenomenon offers another evidence to support the proposal about the existence of a glass skin.

Comparing all of the evidences observed on the investigated glass surfaces, it can be stated that the hydrophilic ions like Na^+ , K^+ etc. play the most important roles resulting in corrosion of glasses in humid air.

4. Conclusion

Glass articles have an SiO_2 -rich skin with smaller network voids, which can sustain the attack of surrounding media. Injury of the skin results in inhomogeneous corrosion products on the surface due to the local ion exchange on the site following the pH increase and subsequent locally limited network dissolution. Consequently many properties of glass



Figures 9a to c. FE-SEM micrographs (Inlens, 1 kV) of the inside of the white glass bottles aged for different periods; a) in air for 9 h, b) in air for one year, c) enlargement of a crystallite in figure 7b.

are changed. The thickness of the skin depends on the cooling rate. In the case of thinner skin, Na^+ ions in the glass migrate easily to the surface and react with the environmental substances to form crystallites of certain shapes. In the case of thicker skin, wax-like droplets are formed on the surface and they etch the skin. Afterwards an inhomogeneous corrosion crystalline pattern appears. The condition of the skin influences the following coatings heavily.

*

Financial support from Freistaat Bayern through WOPAG (Werkstoffverbunde und Oberflächenveredelte Produkte aus Glas) is gratefully acknowledged.

5. References

- [1] Vogel, W.: Glaschemie. Berlin et al.: Springer, 1992.
- [2] Holland, L.: Properties of glass surfaces. London: Chapman and Hall, 1966.
- [3] Dunken, H. H.: Physikalische Chemie der Glasoberfläche. Leipzig: VEB Deutscher Verlag für Grundstoffindustrie, 1981.
- [4] Feldmann, M.; Weißmann, R.: Initial stages of float glass corrosion. *J. Non-Cryst. Solids* **218** (1997) pp. 205–209.
- [5] Hobbs, L. W.: Network topology in aperiodic networks. *J. Non-Cryst. Solids* **192&193** (1995) pp. 79–91.
- [6] Griscom, D. L.: Defect structure of glasses. *J. Non-Cryst. Solids* **73** (1985) pp. 51–77.
- [7] Bunker, B. C.: Molecular mechanisms for corrosion of silica and silicate glasses. *J. Non-Cryst. Solids* **179** (1994) pp. 300–308.
- [8] Schlenz, H.; Kirfel, A.; Schulmeister, K. et al.: Structure analyses of Ba-silicate glasses. *J. Non-Cryst. Solids* **297** (2002) no. 1, pp. 37–54.
- [9] Carter, M. M. C.; McIntyre N. S.; King, H. W. et al.: The aging of silicate glass surfaces in humid air. *J. Non-Cryst. Solids* **220** (1997) no. 2–3, pp. 127–138.
- [10] Creuzet, F.; Guilloteau, E.; Arribart, H.: Characterization of surface defects involved in the fracture of glass. In: Proc. Fundamentals of Glass Science and Technology 1993. 2nd Conf. European Society of Glass Science and Technology (ESG), Venice 1993. Murano: Stazione Sperimentale del Vetro, 1993. Pp. 163–168.
- [11] Wünsche, C.; Rädlein, E.; Frischat, G. H.: Morphology of silica and borosilicate glass fracture surfaces by atomic force microscopy. *Glastech. Ber. Glass Sci. Technol.* **72** (1999) no. 2, pp. 49–54.
- [12] Wünsche, C.; Rädlein, E.; Frischat, G. H.: Glass fracture surfaces seen with an atomic force microscope. *Fresenius J. Anal. Chem.* **358** (1997) pp. 349–35.
- [13] Greaves, G. N.; Smith, W.; Giulotto, E. et al.: Local structure, microstructure and glass properties. *J. Non-Cryst. Solids* **222** (1997) pp. 13–24.
- [14] Hench, L.L.; Clark, D. E.: Physical chemistry of glass surfaces. *J. Non-Cryst. Solids* **28** (1978) pp. 83–105.
- [15] Chen, H.; Park, J. W.: Atmospheric reaction at the surface of sodium disilicate glass. *Phys. Chem. Glasses* **22** (1981) no. 2, pp. 39–42.
- [16] Wiegand, O.; Treuner, A.: Polymerbeschichtungstechnologie von Glasflaschen (WPT-Wiegand-Glas-Polymerertechnologie). In: Ext. Abstr. 72. Glastechnische Tagung DGG, Münster, 1998. Frankfurt/M.: Deutsche Glastechnische Gesellschaft. Pp. 104–107.
- [17] Bianchini, F. G.; Scalet, B.; Verita, M.: SEM and X-ray microanalysis evaluation of tin oxide coatings on hollow glass. *Verres Réfract.* **36** (1981) no. 2, pp. 245–248.
- [18] Schwarzenbach, M. S.: Oberflächen-Charakterisierung pharmazeutischer Glasbehältnisse und Messung verschiedener Wechselwirkungen zwischen Interferon α -2a und Glas. Univ. Basel, Diss. 2001.
- [19] Jang, H. K.; Whangbo, S. W.; Choi, Y. K. et al.: Effects of thermal annealing a glass surface in air. *J. Non-Cryst. Solids* **296** (2001) no. 3, pp. 182–187.
- [20] Kojima, G.; Matsumoto, K.; Sakamoto, O. et al.: Interaction of water with glass at very high temperature under dynamic condition and the properties of the obtained glass surface. *J. Non-Cryst. Solids* **292** (2001) no. 1–3, pp. 50–58.

■ E304P001

Contact:

Dr. Chun Wang
 Lehrstuhl für Physikalische Chemie II
 Universität Bayreuth
 Universitätsstraße 30
 D-95440 Bayreuth
 E-mail: chun.wang@uni-bayreuth.de